Flexural performance of reinforced concrete beams with recycled aggregates and steel fibres

Emmanuel E. Anike, Messaoud Saidani, Adegoke O. Olubanwo and Uchechukwu C. Anya

Original citation:
Anike, Emmanuel E., Messaoud Saidani, Adegoke O. Olubanwo, and Uchechukwu C. Anya. "Flexural performance of reinforced concrete beams with recycled aggregates and steel fibres." In *Structures*, vol. 39, pp. 1264-1278, 2022.
https://doi.org/10.1016/j.istruc.2022.03.089

DOI 10.1016/j.istruc.2022.03.089
ISSN 2352-0124

Publisher: Elsevier

Structures 39 (2022) 1264–1278

Contents lists available at ScienceDirect

Structures

journal homepage: www.elsevier.com/locate/structures

Flexural performance of reinforced concrete beams with recycled aggregates and steel fibres

Emmanuel E. Anike [a,*], Messaoud Saidani [b], Adegoke O. Olubanwo [b], Uchechukwu C. Anya [c]

[a] Centre for Research in the Built and Natural Environment, Coventry University, 3 Gulson Road, Coventry CV1 2JH, United Kingdom
[b] School of Energy, Construction and Environment, Coventry University, Sir John Laing Building, Much Park Street, Coventry CV1 2LT, United Kingdom
[c] School of Engineering and Engineering Technology, Federal University of Technology, P.M.B 1526 Owerri, Imo State, Nigeria

ARTICLE INFO

Keywords:
Recycled aggregate
Precast waste concrete
Concrete mix design
Steel fibres
Adhering mortar

ABSTRACT

The presence of mortar makes recycled aggregate (RA) a heterogeneous material compared to its parallel homogeneous natural aggregate (NA). Consequently, the mix proportioning method most suitable for RA reuse for structural applications has long been debated. This study presents an unconventional mix proportioning method involving recycled fine aggregate (RFA), recycled coarse aggregate (RCA), and steel fibres (SF) for recycled aggregate concrete production. The equivalent mortar volume (EMV) mix proportioning technique developed for concrete containing RCA is extended to incorporate RFA and SF. Five different mixes were formulated using both conventional and the extended EMV mix design methods, to study the flexural behaviour of reinforced concrete beams produced with RA and SF. The results showed that the load bearing capacity of the beam of the mix containing 100% RA and 1% SF prepared using the conventional method, increased by up to 13% and 8% compared to similar mix without SF and the reference mix, respectively. The unconventional beam containing 60% RA showed equal load resistance of 63kN as the reference beam made entirely of NA. Additionally, the unconventional beam had the fewest cracks, least crack width, and visually, the least deflection at the fracture when compared to the other beams with or without SF. This study shows that the extended EMV mix proportioning technique is adequate and offsets the need for SF addition in concrete containing RA.

1. Introduction

Natural aggregate (NA) is diminishing at a faster rate in a bid to meet the global demand for concrete, resulting in an urgent need for alternative sources of aggregates. In Europe alone, aggregates demand is 2.7 billion tonnes on a yearly basis [1]. The recent forecast by the Freedonia group shows that the global demand for construction aggregates will rise 2.3% each year to 47.5 billion metric tons in 2023 [2]. This is expected since aggregates occupy up to 75% by volume of concrete compared to other constituent materials.

At the same time, many existing concrete structures are being demolished following the desire to attain modern designs and specifications [3,4]. The renovation or outright replacement of ageing structures, redevelopment of urban spaces and incidences of natural occurrences such as tsunamis and earthquakes have all contributed to the massive generation of construction and demolition waste (CDW) [5,6]. The common method of handling such construction wastes is to dispose them in landfills. But landfills have become overwhelmed due to the indiscriminate dumping of CDW, leading to environmental hazards. Consequently, the world is confronted with how to protect the diminishing non-renewable NA and the best way to manage the enormous CDW being generated [3]. The way forward is to recycle the waste concretes and use them as aggregates in new concrete [7–9].

The subject of recycling CDW is dated back to the end of World War II [10–13]. The first and second state of the art regarding recycled aggregate (RA) and recycled aggregate concrete (RAC) were published in 1986 [14]. Whereas the first state of the art covers between 1945 and 1977, the second reported investigations from 1978 to 1985. The data contained in the first state of the art were limited, and most of the studies reported were done with RA obtained by crushing concrete used for laboratory experiments. Such version of RA, relatively clean, would definitely show a composition and properties at variant with those of polluted CDW [15–17]. The following conclusions are drawn from the first state of the art:

* Corresponding author.
E-mail address: anikee@uni.coventry.ac.uk (E.E. Anike).

https://doi.org/10.1016/j.istruc.2022.03.089
Received 15 October 2021; Received in revised form 22 March 2022; Accepted 30 March 2022
Available online 8 April 2022

- The presence of crushed concrete fines reduces the workability of concrete considerably, but their influence on compressive strength is little. Conversely, the workability of the concrete mix incorporating recycled coarse aggregate (RCA) is comparable to that of the reference mix consisting entirely of NA.
- The failure of RAC is initiated by the mortar adhering to the RA, hence, the adhering mortar is otherwise known as the weakest link.
- Variation in the elastic modulus of the concrete made of RCA and that of natural aggregate concrete (NAC) is insignificant.
- There are no concerns with respect to concrete resistance to freeze-and-thaw when RA is sourced from an unpolluted concrete.
- Drying shrinkage of RAC is higher than that of NAC.

The second state of the art contains a more detailed information, but in summary, it upheld that the major hindrance in using RA for concrete manufacture is the adhering mortar. However, this problem can be technically resolved. After almost three decades, Silva et al. [18] reviewed a total of 236 publications covering from 1978 to 2014, focusing on both physical and compositional properties of RA. The authors concluded that RA can be likened to a normal aggregate and globally accepted, if it is well processed and classified. Furthermore, the following remarks are drawn from the report:

- The strength properties of concrete produced with RA are negatively influenced by the mixed contaminants associated with CDW.
- A selective demolition approach produces a CDW with less impurity than the comparable conventional method.
- Aggregate size and shape are affected by both crusher type and number of crushing stages; however, the use of jaw crusher gives aggregates of best gradation.
- Recycling procedure, quality of the parent material, and size, all affect mechanical properties of RA.
- RA obtained from concrete alone is of superior quality than those sourced from masonry and CDW.
- In comparison with NA, RA has a lower density and a higher water absorption capacity. This is due to the high porosity of the mortar adhering to the RA.
- As opposed to one transition zone in NAC, there exist two transition zones in RAC, and this is due to the attached mortar. While one transition zone is formed between the original NA and the adhering mortar, another is formed as a result of the interaction between the new and old mortar.

From the foregoing, the downsides of RA for concrete making are induced by the adhering mortar. Dry mortar being a lightweight substance is characterized by high water absorption capacity due to high porosity. As a consequence, according to Wardeh et al. [19], an additional water is required for RAC mixes to achieve a similar workability with their corresponding NAC mixes, and such alteration may impact on the mechanical properties of the RAC. Efforts have been made to remove the adhering mortar, including chemical process [20–22] and thermal process [23–26]. But whereas the former introduces chloride and sulphate ions (which are detrimental) into the raw material, the latter uses a high amount of thermal energy, resulting in the emission of carbon (iv) oxide. On the other hand, some researchers proposed the use of certain percentages of RA as replacements for NA [27–29], to normalize RA. This idea of partial substitution with RA limits the full-scale integration of concrete waste in the production of concrete [30]. Other techniques suggested include, but are not limited to, altering the water-to-cement ratio of the concrete mix [31,32], different mixing methods such as two-stage mixing approach (TSMA), mortar mixing approach, and sand enveloped mixing approach [33–35], and the inclusion of fibres in RAC mixes [36–40].

The use of fibres in RAC mixes has become popular due to their influence on concrete responses to compressive, tensile, and flexural forces, as well as crack development. In terms of compressive strength, however, some authors reported an increase by fibre addition [41–45], while others noted a significant reduction [46–50]. This contrasting result may be attributed to varied fibre contents used, as "balling" effect is expected in the concrete mix with a high fibre content, which ultimately would impair concrete strength [7]. Other mechanical properties, including tensile and flexural strengths, of fibre-reinforced concrete are generally improved. Vaishali and Rao [36] studied the performance of three different types of fibres, namely; glass, polypropylene and steel fibres. The authors concluded that steel fibre (SF) had the greatest influence and that improvement by fibres was more in RAC than NAC. They also endorsed the use of both RFA and RCA in high performance concretes, provided that the volume of SF is restricted to 1%.

Remarkably, until 2009, conventional mix proportioning methods were used to formulate RAC mixes in most research (if not all). Using such methods developed for concretes containing homogeneous NA, would assume the heterogeneous RA as uncontaminated. The implication, therefore, is that the overall mortar content of the RAC mix would be higher than that of its comparable NAC proportioned with similar method [51]. Hence, Fathifazl et al. [52] proposed the "Equivalent mortar volume (EMV)" mix proportioning technique, which considers the adhering mortar as part of the total mortar content in RAC. This method uses the actual properties of the RA to determine the right replacement ratio, eliminating the use of *trial-and-error* method (percentage replacements) suggested in the literature. In addition, the potential risk of any undesirable properties of RA with no history data or from variety of sources pointed out by Bravo et al. [16], is prevented. Another group of researchers proposed an optimization-based technique referred to as particle packing method (PPM), which aims at maximizing packing density of RCA, thereby minimizing the void content in RAC [53].

The structural performance of RAC beams was enhanced using the EMV and PPM methods compared to the conventional method [53–55]. With respect to crack pattern and morphology, Pradhan et al. [55] observed that there was no significant difference between reinforced beams of NAC and RAC, but the authors noted that the RAC beam samples exhibited higher number of cracks than their equivalent NAC samples. Similarly, Arezoumandi et al. [56] reported that RAC and NAC beams tested in flexure showed similar crack development but not crack spacing. The presence of SF improves the flexural strength of RAC [39,41]. Up to 15% increase in flexural strength was noticed by using 2% (by mass of concrete) SF in RAC compared to NAC with no SF [41]. The results of an experimental study carried out with RCA derived from demolished old concrete bridge and discarded laboratory concrete samples showed that the flexural performance of reinforced RAC beams under short-term loading, were satisfactory for both service and ultimate loading, compared to NAC beams [57].

To the best of the present authors' knowledge, no study to date, has used any known unconventional method to proportion RAC mixes involving RFA, RCA, and SF. Because RFA constitutes a larger proportion of the crushed concrete than the corresponding RCA, its use in concrete production would ensure an absolute solution to the environmental impacts of waste concrete. Consequently, the EMV mix proportioning technique developed for concrete containing RCA, was extended in this work to incorporate RFA. On the other hand, the addition of SF in RAC mixes is deemed necessary to compensate for loss of strength. The flexural behaviour of the reinforced concrete beams produced using this extended EMV approach, were studied alongside other beams, by examining the mid-span deflection, failure load and mode, crack initiation and development, strains, and crack width (at the fracture). Also, compressive strength, tensile splitting strength and hardened density of the concretes were investigated experimentally.

2. Theory

RA derived from waste concrete can reduce the pressure on diminishing NA and the environmental challenges arising from construction and demolition activities, if an appropriate mix design method is adopted for RAC. Although the quality of the RA obtained from waste concrete depends on the strength of the parent concrete, recycling process, and particles size [10,18,58], as well as the extent of contamination. In the writers' opinion, precast waste concrete at a production facility site is of high-quality and has not undergone any deterioration, as such, the RA sourced from them can replicate similar results as NA in concrete. This view has been expressed by early authors who maintained that concrete wastes generated from new construction, repair, renovation, and demolition, contain more impurities than those generated from precast waste described to be of a superior quality and free from impurities [59–61]. Therefore, RA from precast waste concrete is believed to be capable of replacing both fine and coarse aggregates in concrete, without adverse effects on concrete properties, provided that the adhering mortar is accounted for during the mix design.

Upon the foregoing, this work was stimulated. To verify these assumptions, a large-scale experimental campaign was undertaken to examine the mechanical properties of concretes prepared with RA (RFA + RCA) from precast waste concrete, using both conventional and the extended EMV mix proportioning methods. The properties of concretes consisting of partial and full replacements with RA were compared to those of the reference mix made entirely of NA. The full description of the "Extended EMV" technique is given in an earlier study by the authors [3].

3. Materials and method

3.1. Materials

3.1.1. Aggregates

The NA used in this study was the original aggregate in the parent concrete from which the RA was obtained. The RA was derived from condemned precast concrete beams manufactured by Litecast Homefloors Ltd, Nuneaton, United Kingdom. The information provided by the company showed that the parent concrete had an average cube compressive strength of 40 MPa after 24 h. The concrete rubble was crushed in a Master Compact Crusher 70Go!™ and sieved into fine and coarse aggregates. The aggregates were then stored in a 60-Litre Plastic Barrels, according to grades (see Sections 3.1.1.1 and 3.1.1.2). The moisture content of the aggregates in each container was determined and used for the concrete mix design, accordingly. Important properties required to characterize all aggregates were determined according to relevant standards given in Table 1. The results of the sieve analyses of both natural and recycled aggregates are given in Fig. 1.

3.1.1.1. Fine aggregates. All aggregates with nominal diameter less than 4.75 mm were regarded as fine aggregates for both NA and RA. The aggregates are presented in Fig. 2 and their properties are given in

Table 1
Standard for the characterization of aggregates.

Property	Standard
Sieve analysis of fine and coarse aggregates	ASTM C136/C136M–14 [62]
Bulk density and voids in aggregate	ASTM C29/C29M–17a [63]
Specific gravity and absorption of fine aggregate	ASTM C128–15 [64]
Specific gravity and absorption of coarse aggregate	ASTM C127–15 [65]

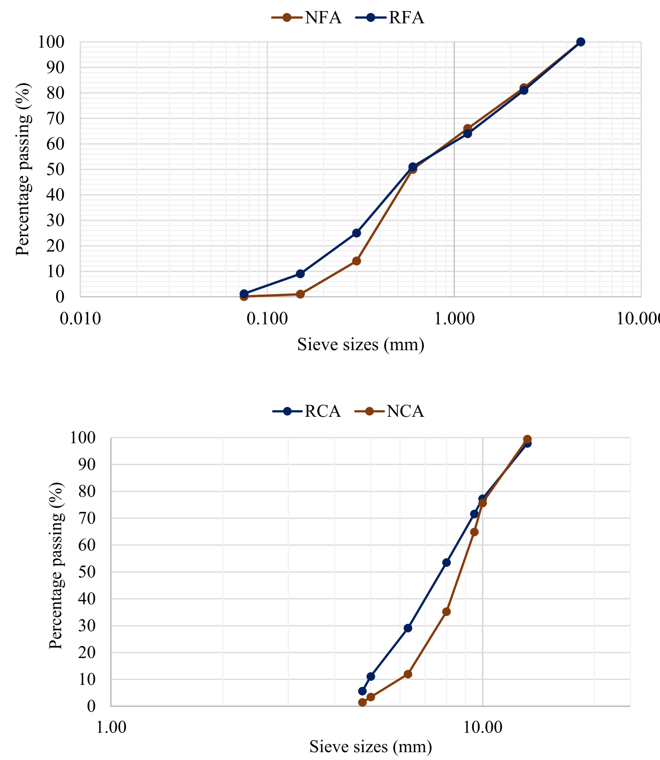

Fig. 1. Grain size distribution of the aggregates.

Table 2. Because the grain size distributions of the ungraded natural and recycled fine aggregates varied widely, the aggregates were sieved through a set of wire mesh in the order of nominal apertures: 2.47 mm, 0.57 mm, and 0.075 mm, to obtain a medium range fineness modulus. The particles that passed through the 0.075 mm sieve were discarded. The combining ratio that gave a similar fineness modulus of 2.87 and 2.71 for natural fine aggregate (NFA) and RFA respectively, was 1:2:3 (corresponding to 2.47 mm:0.57 mm:0.075 mm). It is worth mentioning that the fineness modulus of the ungraded RFA was found to be 3.25.

Generally, the specific gravity of RFA was found lower compared NFA as shown in Table 2. It can also be observed that the specific gravity of the RFA increases with increasing particles size, while that of the NFA shows an inverse relationship with the particles size. The oven-dry and saturated surface-dry specific gravity of the NFA are respectively 14.3% and 23% greater than those of the RFA. The average absorptions of RFA and NFA are 13.0% and 1.0% respectively. Whereas the absorption of the NFA decreases with particles size, that of the RFA increases as particles size reduces. This can be attributed to high mortar content present in RFA produced during the crushing process.

3.1.1.2. Coarse aggregates. Aggregates of maximum grain size 14 mm which were retained on 4.75 mm sieve, were taken as the coarse aggregates for both NA and RA. The aggregates were graded into two by sieving them through 4.75–10.00 mm and 10–14 mm sieves. In this study, all concrete mixes contained 70% and 30% of 4.75–10.00 mm and 10–14 mm grades, respectively. The natural coarse aggregate (NCA) and RCA are as presented in Fig. 2 and their properties are given in Table 2. Unlike their fine aggregate counterparts, the specific gravity of both RCA and NCA are not affected by grain size.

However, the NCA has a higher specific gravity compared with RCA. The water absorption capacity of both NCA and RCA decreases as particles size increase, with average values of 0.8% and 5.3% respectively.

3.1.2. Cement, water, and superplasticizer

CEMEX Rapid CEM I Portland cement conforming to the British standard BS EN 197–1 [66] was used. The physical, chemical, and

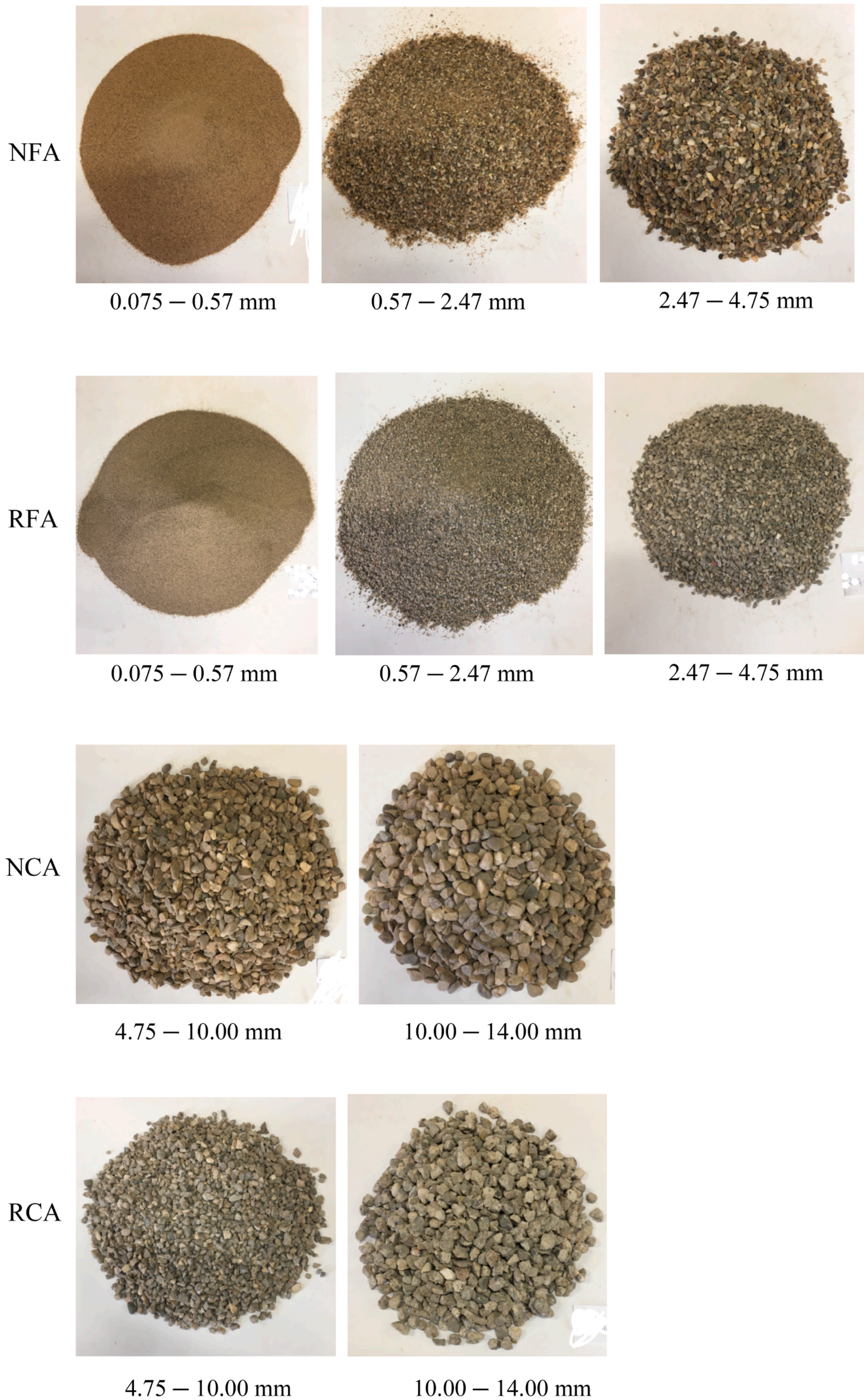

Fig. 2. Natural and recycled aggregates used in this study.

mechanical properties of the cement, provided by Rugby CEMEX UK Cement Limited, for an average of four set of tests, are given in Table 3. Potable water obtained from the laboratory was used. A modified polycarboxylate high range superplasticizer known as Sika ViscoCrete 335, was used to achieve the desired workability of the concrete mixes. The product specification conforms to BS EN 934–2 [67] and its technical data showed a density of 1.08 kg/l (at + 20 °C) and maximum alkali content of 0.25%.

3.1.3. Steel fibres

Three types of SF, all made of the same material composition but differ in geometry as shown in Fig. 3, were employed in this study. The length and diameter of the SF are 60 mm and 1.0 mm diameter respectively, resulting in an aspect ratio of 60. They have a common tensile strength of 1900 MPa, and chemical composition given in Table 4.

Table 2
Physical and mechanical properties of natural and recycled aggregates.

Aggregates		Specific gravity		Density (kg/m^3)		Water absorption (%)	Void (%)	Mortar volume (%)
type	size fraction, d (mm)	OD	SSD	Dry-rodded	Loose bulk			
NFA	$0.075 \le d \le 0.57$	2.62	2.64	–	–	0.6	–	–
	$0.570 \le d \le 2.47$	2.57	2.60	–	–	1.1	–	–
	$2.470 \le d \le 4.75$	2.48	2.52	–	–	1.4	–	–
RFA	$0.075 \le d < 0.57$	1.78	2.10	–	–	18.1	–	–
	$0.570 \le d \le 2.47$	1.96	2.20	–	–	12.1	–	–
	$2.470 \le d \le 4.75$	2.15	2.34	–	–	8.9	–	–
NCA	$4.750 \le d \le 10.0$	2.60	2.63	1543	1450	0.9	41	–
	$10.00 \le d \le 14.0$	2.62	2.64	1586	1479	0.6	39	–
RCA	$4.750 \le d \le 10.0$	2.30	2.42	1300	1207	5.4	43	51.5
	$10.00 \le d \le 14.0$	2.30	2.42	1293	1171	5.1	44	52.0

OD; oven-dry, SSD; saturated surface-dry.

Table 3
Physical/Chemical/Mechanical properties of cement.

Fineness (m^2/kg)	–	527
Initial setting time (mins)	–	96
Expansion (mm)	–	0.8
Loss on ignition (%)	–	2.86
Alkalis $(Na_2O)_e$ (%)[§]	–	0.65
Chloride as Cl (%)[ł]	–	0.05
Compressive strength (MPa)[γ]	2 days	38.9
	7 days	51.5
	28 days	62.7
Chemical composition (%)	SiO_2	19.99
	Al_2O_3	4.75
	Fe_2O_3	2.91
	CaO	63.77
	MgO	1.13
	SO_3	3.56
	$Na_2O_{(eq)}$	0.65
	Cl	0.05
	FL	2.02
	C_3S	47.84
	C_2S	26.3
	C_3A	8.33
	C_4AF	9.67

[§] Average of 25 data with a standard deviation of 0.03; [ł]Average of 25 data; [γ]According to BS EN 196–1.

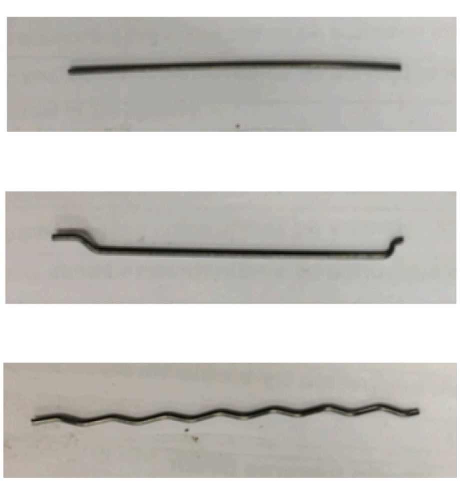

Fig. 3. Steel fibre types investigated.

3.2. Concrete mixtures

A total of five principal concrete mixtures were designed using both conventional method and the extended EMV technique. All the mixes were designed to have 40 MPa target strength, effective water-to-cement ratio of 0.42 and are summarized as follows:

Table 4
Chemical composition of SF.

Elements	Composition (%)
C	0.7
Si	0.22
Mn	0.55
P	0.015
S	0.006
Cr	0.02
Ni	0.01
Cu	0.03
Fe	Balance

(i) Natural aggregate concrete (NAC)—This was the reference mix consisting of NA and designed using the conventional method.
(ii) Recycled aggregate concrete (RAC)—Both fine and coarse aggregates in this mix were recycled, and the mix was designed with conventional method.
(iii) Steel fibre-reinforced recycled aggregate concrete (SFRRAC)—This comprised of the mix in (ii) and the optimum SF volume ratio appropriate to the conventional mix design method.
(iv) Blended aggregate concrete (BAC)—This mix consisted of both natural and recycled aggregates and was proportioned using the extended EMV mechanism. The replacement level with RA depended on the mortar content of the RCA as described in Section 3.3.2.
(v) Steel fibre-reinforced blended aggregate concrete (SFRBAC)—This composed of the mix in (iv) and the optimum SF content appropriate to the extended EMV mix proportioning method.

3.2.1. Preliminary study

Rial mixes were designed and examined experimentally to attain the desired workability (measured using a slump test) for the concrete mixes stated in Section 3.2. Concretes for structural purposes are expected to be consistence class S3 and the slump for class S3 is in the range 90–170 mm [68,69]. Also, the optimization of SF content appropriate to each mix design method adopted was conducted. This was done by introducing SF volume fractions 0.125% to 1.50% in the concrete mixes and testing some cube specimens under compression after curing in water for 7 days. Furthermore, the three types of SF adopted for this study were investigated at this stage, to determine the one that best improves concrete strength. In addition, two conventional mix proportion methods given by the American Concrete Institute (ACI) [70] and the Department of Environment (DoE) [71] were both assessed experimentally. This was with the intention of determining the approach that managed resources better without compromising concrete strength at the same time. The details of the preliminary study have been published by the authors [3,72].

In summary, the studies showed that the undulated SF offered the best improvement than its straight and hooked-ended counterparts. The optimum SF volume ratios suitable for the mixes proportioned with the conventional and the extended EMV methods were 1.0% and 0.5%, respectively. Also, the ACI mix design method performed better than its equivalent DoE approach, hence, the former was adopted for the present investigation.

3.3. Mixture proportioning approaches

3.3.1. Conventional method

The absolute volume mix design method given by the ACI Committee 211 [70] was used to proportion the NAC, RAC, and SFRRAC mixes. In this method, the RA was simply treated like its parallel NA with no special consideration for the presence of the adhering mortar. However, the mixing process of the mixes containing RA was different from those constituting entirely of NA as shown in Fig. 4. All cubical and cylindrical specimens were compacted in layers, regardless of mix proportioning method, to achieve full compaction. Vibrating table was used for the cubes and cylinders, while needle vibrator was used for the reinforced concrete beams. Concrete cubes and cylinders were cured in water by immersion for the required age (7, 28, and 56 days) whereas the beams were cured in air at room temperature for 28 days.

3.3.2. Equivalent mortar volume (EMV) method

According to the EMV guidelines, the replacement ratio of NCA with RCA depends on the residual mortar volume (RMV) of the RCA and a series of mathematical calculations are involved in the mix design. In line with the EMV mix design provisions, the maximum theoretical RMV of the RCA can be obtained using the following expressions:

$$RMV_{max}\% = \left[\frac{SG_b^{RCA} - \left(V_{DR-NCA}^{NAC}\right)\left(SG_b^{NCA}\right)}{SG_b^{RCA}}\right] \times 100 \quad (1)$$

where V_{DR-NCA}^{NAC}, SG_b^{NCA}, and SG_b^{RCA} are the dry-rodded volume of NCA in NAC, bulk specific gravity of NCA, and bulk specific gravity of RCA, respectively.

There is a possibility of total replacement of the NCA with RCA, only if the maximum theoretical RMV obtained from Eq. (1) is greater than

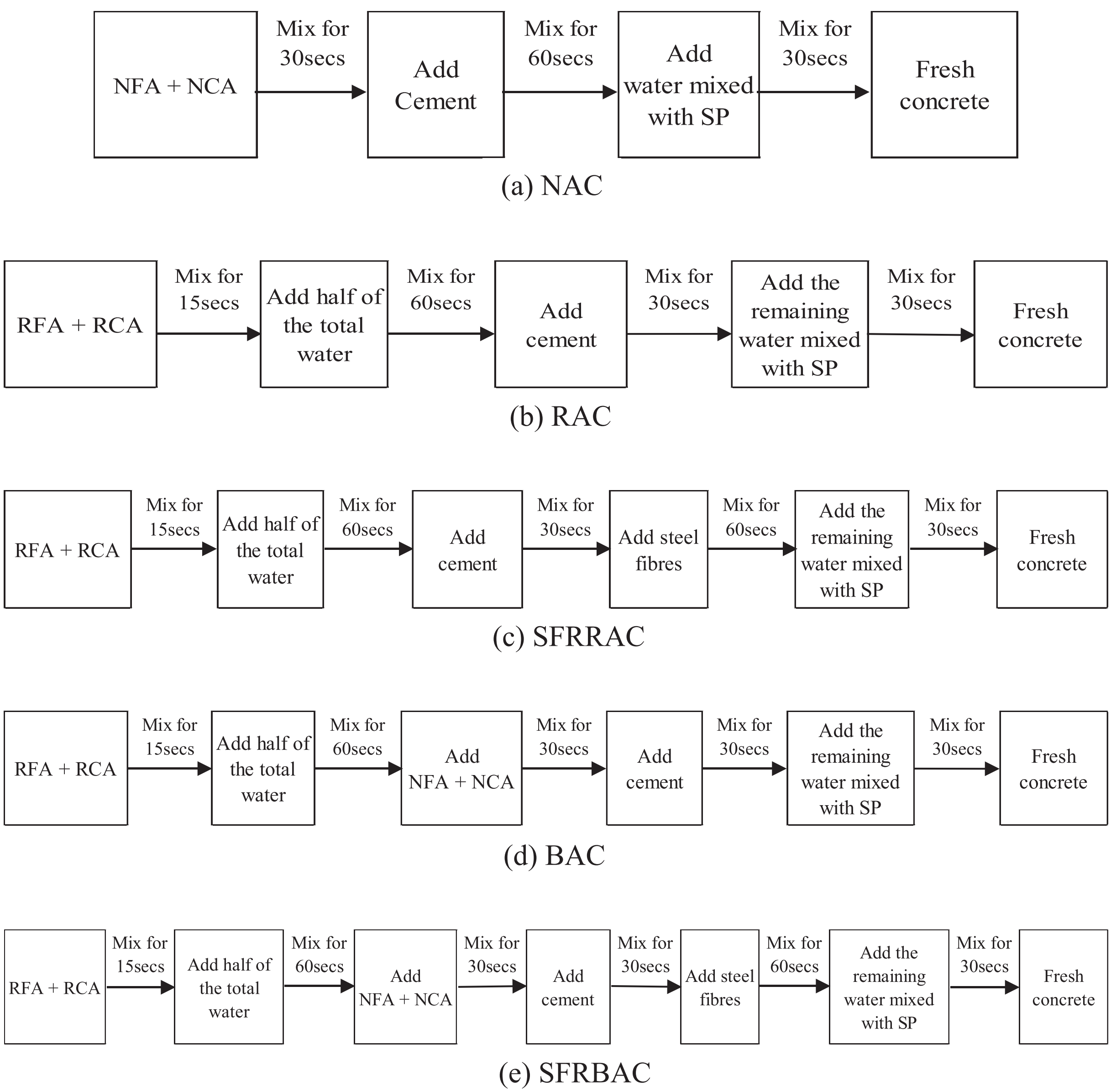

Fig. 4. Mixing processes for different concrete mixtures.

the actual (experimental) RMV of the RCA, otherwise, not viable. Applying a similar procedure adopted by Abbas et al. [51], the actual RMV of the RCA used in this study was found to be 52%. Using Eq. (1) and necessary substitutions, the maximum theoretical RMV was 37.6%. Thus, the viable replacement ratio with RCA was 60% and this ratio was also applied to the RFA. The mixing procedures for the BAC and SFRBAC mixes developed from the extended EMV guideline are illustrated in Fig. 4. The resulting mix proportions studied, based on oven-dry condition of the aggregates, are presented in Table 5.

3.4. Specimens and testing

An average of 5 cube specimens (100 × 100 × 100 mm) were prepared from each mix and tested for hardened density according to BS EN 12390–7 [73] after 7, 28, and 56 days of curing. Subsequently, the specimens were subjected to compression test in accordance with BS EN 12390:3 [74] using an automated 2000kN bearing capacity Avery-Denison compression testing machine. A constant loading rate of 8kN/s was applied on the specimens until failure occurred. The same machine was used to test for tensile splitting strength in accordance with BS EN 12390–6 [75] using an average of 3 cylindrical specimens (150 mm diameter × 300 mm high) prepared from each mix after 28 days of curing. The application of load was done at a constant rate of stress of 0.05 N/mm^2·s. Flexural behaviour of NAC, RAC, SFRRAC, and BAC beams were investigated using 80 × 180 × 1500 mm specimens, in which two specimens were fabricated from each mix, cured, and subjected to a four-point bending and simply supported test to determine the ultimate load, strains, mid-span deflections, and crack patterns of the reinforced concrete beams.

3.5. Instrumentation, test setup and procedures

Rebars of size 10 mm and stirrups of size 8 mm were used to produce the beam specimens. For each beam, two 10 mm reinforcements and ten two-legged stirrups (five at each end spaced at 20 mm centre-to-centre), shown in Fig. 5 were used. Concrete cover of 20 mm to the reinforcements was achieved using six rubber spacers placed alternately at the bottom of the two reinforcements. In order to reveal crack initiation and propagation during the testing, one side of each beam was first cleaned of any grits and painted white prior to the day of testing. On the painted side, a vertical line was drawn at the centre of the beam which divided it into two equal halves. A total of five DEMEC buttons were installed on each side of the centre line, with the aid of glue, to measure the surface strains. The horizontal and vertical distances separating the DEMEC buttons were approximately 200 mm and 40 mm, respectively.

Table 5
Concrete mix proportions.

Concrete constituents (kg/m^3)	Concrete mixture				
	NAC	RAC	SFRRAC	BAC	SFRBAC
Water	213	213	213	153	153
Cement	507	507	507	364	364
w/c	0.42	0.42	0.42	0.42	0.42
NFA	707	0	0	203	203
RFA	0	534	534	305	305
NCA	856	0	0	493	493
RCA	0	754	754	754	754
SP	1.27	1.52	3.8	7.28	12
SF	0	0	78.5	0	39.25
Slump (mm)	110	135	135	170	170
Design method	ACI	ACI	ACI	EMV	EMV

w/c; water-to-cement ratio, SP; superplasticizer.

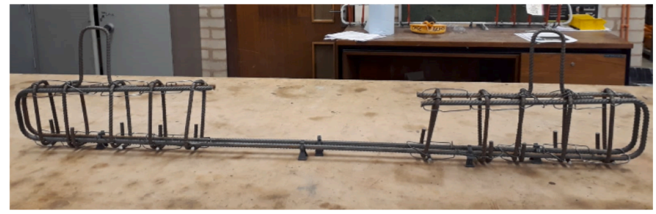

Fig. 5. Arrangement of reinforcements, stirrups, and rubber spacers.

Each specimen was then positioned in the testing equipment maintaining a clear distance of 1200 mm between the two supports. The schematic of the test setup for the flexural behaviour is as illustrated in Fig. 6(a) and the central cross-sectional area of the beams is shown in Fig. 6(b), in which $b = 80mm$, $h = 180mm$, $A_s = 157.8mm^2$ and y differ for the various mixes studied. Where b, h, A_s, and y are the width of the beam, overall depth of the beam, cross-sectional area of the of the steel reinforcements, and neutral axis depth, respectively. A 1000kN servo-controlled hydraulic actuator attached to a rigid frame was used to apply the load at 5kN increments and rate of 200 N/s. Before the load application, the DEMEC readings (with no loads) were noted, and the mid-span deflection was automatically zero. Subsequently, the DEMEC readings at the incremental load were taken and recorded. While the DEMEC readings were taken using a DEMEC gauge, the corresponding mid-span deflection was read from the computer screen with data logger with an electronic linear variable displacement transducer (LVDT). A gauge factor of 0.403 × 10^{-2} was used to multiply each of the DEMEC readings and the gauge reading at every load-step was subtracted from the initial reading (with no loads) to obtain the concrete strain.

The load at the first cracks appearance was noted and the cracks were amplified with coloured marker and the longest crack at every load-step was traced using a thread and measured with a ruler. Upon additional loads, the propagation of cracks was magnified with different colours of marker and measured accordingly. The corresponding load producing the cracks were labelled beside them and the load was sustained until failure occurred. The ultimate load, failure mode, and estimated crack width were all recorded.

According to Megson [76], the second moment of area about the neutral axis for composite analysis using transformed area method, is given by:

$$I = by^3/3 + mA_s(d-y)^2 \tag{2}$$

where m is the modular ratio (the ratio of the elastic modulus of steel to that of concrete) and d is the effective depth of the beam. Also, for concrete beam of a rectangular section, Megson [76] gave the moment of resistance, M_r as:

$$M_r = f_c/2\, by(d - y/3) \tag{3}$$

where f_c, is the compressive strength of the concrete. Theoretically, from Fig. 6(a), the ultimate moment, M_{ult} will occur under the point loads acting 400 mm from either supports of the beam. This can be expressed mathematically as:

$$M_{ult} = Pa/2 \tag{4}$$

The load value at which the induced moment (Equation (4)) equals the beam moment of resistance (Equation (3)) is the theoretical failure

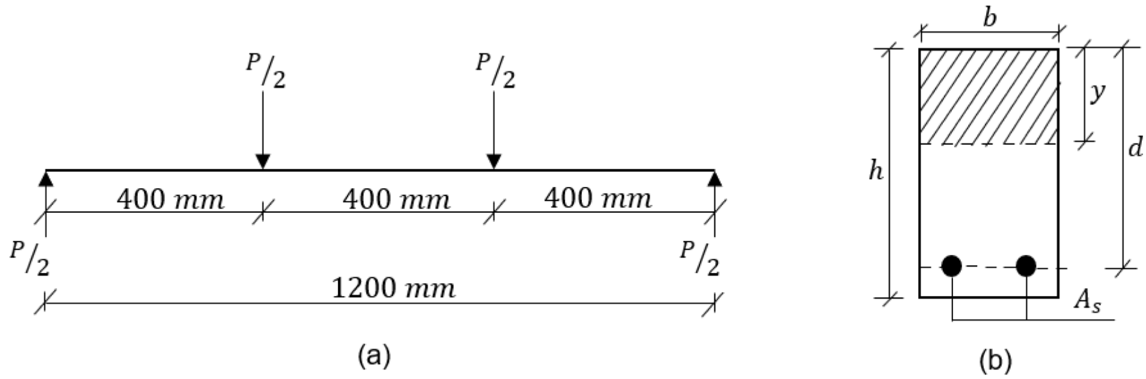

Fig. 6. Idealised equipment setup for the four-point bending test and the central cross section of the reinforced concrete beams.

Table 6
Density of Hardened Concrete.

Age (days)	Average density (kg/m^3)				
	NAC	RAC	SFRRAC	BAC	SFRBAC
7	2381	2178	2228	2324	2340
28	2363	2182	2238	2358	2370
56	2366	2185	2235	2327	2360

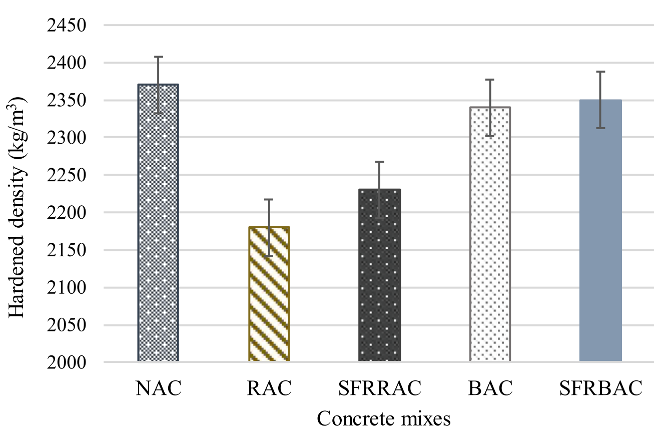

Fig. 7. Average density of hardened concrete showing the influences of RA, SF, and mix proportioning method.

load [77]. Therefore, the ultimate theoretical load, P_{ult} can be expressed as:

$$P_{ult} = 2M_r/a \tag{5}$$

Substituting the dimensional values of the transformed beam section and the modular ratios into Equations (2)–(5), the theoretical values of M_{ult} and P_{ult} for all the mixes studied were obtained, presented, and compared with their experimental counterparts in Table 7. The details of the calculations are given in Appendix A.

4. Results and discussion

4.1. Hardened density

Table 6 shows the density of hardened concrete from the five mixes studied, measured at 7, 28, and 56 days. The density of hardened concrete was determined at these ages because compressive strength was required at the periods. However, since density does not change with age, the average density of fifteen specimens for each mix was plotted in Fig. 7. Obviously, Fig. 7 shows that the addition of SF improved the density of hardened concrete despite the mix proportioning method. This is evident when the densities of SFRRAC and SFRBAC are compared to those of RAC and BAC, respectively.

In general, the hardened density of RAC consisting of 100% RA and proportioned using the traditional method was reduced by 8% compared with that of NAC. This variation was reduced to 6% when SF was introduced to the RAC mix. Using the extended EMV mix proportioning technique, however, only 1% difference was observed between the hardened density of BAC and NAC mixes, in favour of the latter. Further reduction to 0.8% was recorded in the density of concrete when SF was added to BAC mix (that is, the SFRBAC mix). The density of the BAC mix showed up to 7% higher value than that of the RAC mix.

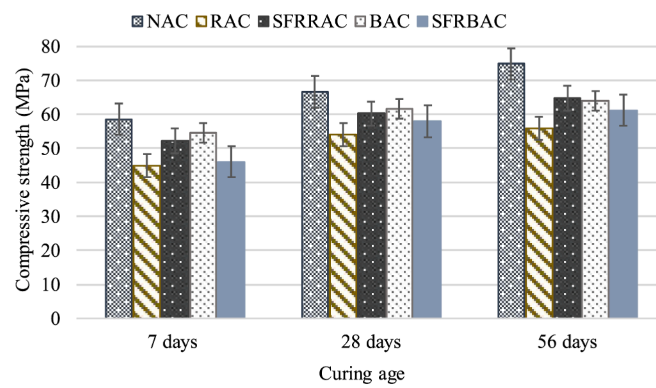

Fig. 8. Effect of curing age on the compressive strength of concrete.

4.2. Compressive strength

The compressive strength of concrete was affected by curing age, aggregate type, RA content, SF addition, and mix proportioning method as shown in Fig. 8. The compressive strength of concrete improved with curing age regardless of the mix proportioning method and aggregate type used. This was expected due to hydration process of the cement composite. The reference mix showed a higher compressive strength than the corresponding mixes containing RA, irrespective of the replacement level with RA, presence of SF, or mix design method. In comparison with NAC mix, the difference in compressive strength of RAC, SFRRAC, BAC, and SFRBAC mixes measured at 7 days was 23.5%, 10.8%, 7%, and 12.9%, respectively. These gaps were substantially reduced at 28 and 56 days. This is because the rate of strength development is higher in concrete containing RA than in normal concrete [78,79], as a result of further hydration reaction induced by the residual mortar [80].

In terms of substitution ratio with RA, the BAC mix consisting of 60% RCA and RFA showed up to 17.8%, 12.5%, and 12.5% greater compressive strength at 7, 28, and 56 days respectively than the comparable RAC made of 100% RA. It can therefore be concluded that the compressive strength of concrete decreases as the RA content increases. This is in agreement with the findings of previous researchers [29,81].

The compressive strength of the RAC mix proportioned with conventional method was enhanced by the introduction of SF as shown in Fig. 8. Similar findings have been reported in the past [41–45]. The bridging effect of SF which prevented the propagation of micro-cracks was responsible for the improvement. Additionally, it was reported that the hydration reaction of the paste was promoted by the presence of SF and more complete compared to concrete with no SF [37]. This study, however, showed that the influence of SF on the compressive strength depended on SF content and mix proportioning method adopted. The presence of SF in the SFRBAC mix resulted in a harsh mix (due to high coarse aggregate content), thereby reducing strength.

Using the extended EMV mix proportioning approach resulted in a remarkable improvement on the compressive strength of the concrete. Even though the cement content in the NAC mix was significantly higher than that of the BAC mix, there was only 7% difference in their compressive strength in favour of the reference mix. This impressive outcome of the BAC mix was due to higher dosage of superplasticizer and improved particle packing. According to Moosberg-Bustnes et al. [82], the use of superplasticizer induces a loose but more homogeneous particles packing in the concrete matrix. Table 5 shows that the BAC mix contained a higher amount of superplasticizer relative to the RAC mix. It has also been reported that RCA has a lower packing density than NCA due to the mortar adhering to the RCA [19]. Therefore, the BAC containing 60% RA is expected to have a higher packing density than the equivalent RAC consisting of 100% RA. Since concrete properties are enhanced by packing density [53], the BAC showed a higher strength.

Comparisons of results were made between the present study and previous investigations where the EMV method was used to design the concrete mix incorporating just RCA. Gupta and Bhatia [83] reported a higher compressive strength for the concrete prepared with RCA using the EMV guide compared to the conventional concrete. Up to 13% greater strength was observed for the recycled concrete proportioned with the EMV procedure than the normal concrete [52]. In the current study, the BAC mix proportioned using the extended EMV technique, did not achieve a higher compressive strength than the NAC. This may be due to the presence of RFA in the BAC mix, and the fact that the quality of the RCA used here differ from those of the previous works as shown in the reported residual mortar contents of their RCA.

4.3. Tensile splitting strength

According to Fig. 9, all mixes consisting of RA showed a higher tensile splitting strength than the reference mix, despite the substitution ratio with RA. This agrees with the results published by early researchers [39,84–86]. The tensile splitting strength of RAC mix made of 100% RA was 4.05 MPa, while its comparable NAC consisting of 100% NA was 3.80 MPa. The BAC showed a tensile splitting strength of 4.30 MPa, exhibiting up to 6% and 12% more strength than the parallel RAC and NAC, respectively. Fathifazl et al. [52] reported a similar result of 11% higher strength for the RAC proportioned with the EMV method than the conventional concrete. It can be deduced that RA content has a minimal effect on this property of concrete. This confirms the position of previous authors who maintain that the tensile strength of the RAC depends on the quality of RA rather than the amount used [5,59,85].

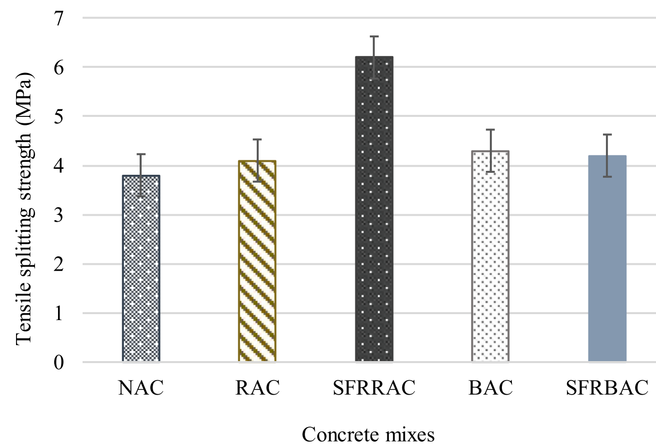

Fig. 9. Tensile splitting strength of concrete at 28 days.

The results presented in Fig. 9 also show that the tensile splitting strength of the mixes incorporating SF is significantly higher than those of other mixes. This was expected due to the ability of SF to bridge cracking propagation, thus sustaining more load prior to failure. According to Akinkurolere [87], post-cracking resistance and toughness of concrete are improved by SF. Although SFRRAC showed up to 33% improvement over the RAC, there was no substantial difference between the tensile strength of SFRBAC and BAC. In fact, the inclusion of SF led to a slight decrease in the tensile splitting strength of SFRBAC compared to BAC. The reason is because the BAC mix (with a high volume of coarse aggregate) became harsh when SF was added, leading to strength reduction.

4.4. Flexural behaviour

4.4.1. Ultimate load

Table 7 shows that the SFRRAC had the highest load bearing capacity compared with NAC, RAC, and BAC beams. The SFRRAC beam consisting of 100% RA showed up to 8% greater load capacity than the comparable NAC (reference) beam. The results also show that the effect of SF on the load capacity of the concrete beams containing RA, increased above 13% when the RAC and SFRRAC mixes are compared. Evidently, the RAC beam had the least resistance to the applied load, and this was due to the RA content in the mix. There was about 6.3% deficiency in the load resistance of the RAC beam relative to its corresponding NAC beam.

However, using an alternative to the conventional mix proportioning method enhanced the ultimate load capacity of concrete made of RA. In Table 7, the BAC mix proportioned with the extended EMV method, produced beams with up to 6% higher load capacity than the parallel RAC mix. There was no significant difference in ultimate load between the BAC and NAC beams. It is noteworthy that the cement content of the BAC mix was substantially lower (143 kg per m^3 of concrete) compared to those of the RAC, SFRRAC, and NAC mixes.

4.4.2. Cracking development and failure mode

Fig. 10 shows the cracking pattern of all the beams tested. In terms of crack initiation, the RAC beams had their first cracks at 15 kN load while those of other beams occurred at 20 kN load. The average number of first

Table 7
Summary of results for the beams.

Mix ID	Ultimate load, P_{ult} (kN)			Ultimate moment, M_{ult} (kNm)			Mid-span deflection¶, δ (mm)	Estimated crack width†, (mm)
	E_P	T_P	E_P/T_P	E_M	T_M	E_M/T_M		
NAC	63.7	74.0	0.86	12.7	14.8	0.86	8.47	4.0
RAC	59.7	62.3	0.95	11.9	12.5	0.95	7.60	3.5
SFRRAC	69.0	68.1	1.01	13.8	13.6	1.01	11.75	3.0
BAC	63.4	69.5	0.91	12.7	13.9	0.91	10.37	1.0

Note: E and T mean experimental and theoretical respectively; ¶Deflection at the load step before failure occurred †Crack width at failure.

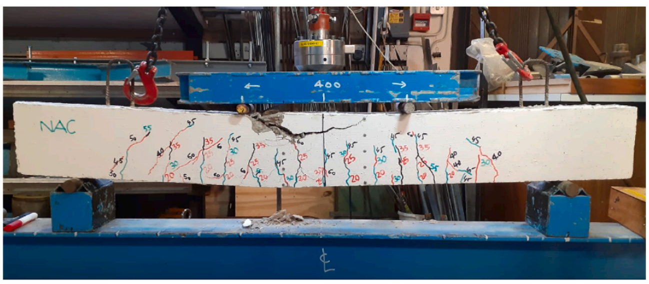

(a) NAC

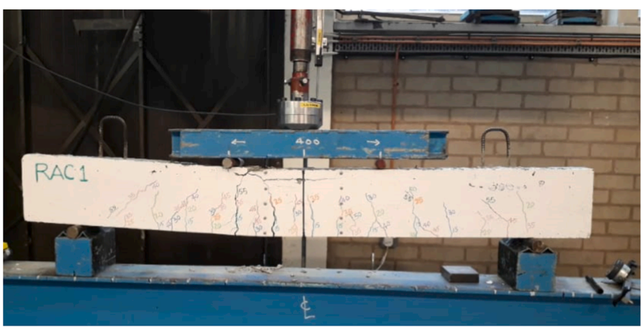

(b) RAC

(c) BAC

(d) SFRRAC

Fig. 10. Crack patterns of the beams under four-point bending and simply supported test.

cracks observed was 10, 9, 3, and 4 for the NAC, RAC, BAC, and SFRRAC beams, respectively. The corresponding longest of these first cracks measured were 70 mm, 97 mm, 60 mm, and 56 mm, respectively. It must be stated that for all the samples, cracks emanated from the tensile zone (bottom) of the beam and their nature was hair-like. The cracks staggered upwards from the bottom, concentrating mostly toward the middle-third of the span of the beams, and were all flexural as indicated in Fig. 10(a)–(d). More cracks developed and spread within the span of the beams as the load intensity was increased, leading to shear cracks which migrated from the support region and progressed toward the nearest point load.

The concrete in the compression zone (top) of the beams crushed as the load intensity was sustained, then failure was induced. Typically, the neutral axis depth kept reducing following cracks development upon load application, resulting in a corresponding reduction of the compression zone. The steel reinforcements yielded first, followed by a localized crushing of the concrete (in the vicinity of the point load) in the compression zone as shown in Fig. 10. This type of failure is normally regarded as a ductile mode of failure.

Although the nature of cracking propagation in the NAC, RAC, and BAC beams containing no steel fibres was similar, the BAC beam had fewer and lesser severe cracks (both before and at failure) than all the other beams including the SFRRAC beam. This was due to a higher content of coarse aggregate in the BAC mix compared to other mixes. Previous researchers observed that when a concrete beam was subjected to flexural testing, cracking propagation was impeded by coarse aggregates and the cracks found a path of lowest resistance round the aggregates [88]. Additionally, the BAC mix constituted a greater volume of superplasticizer (which offers a better particle packing density in concrete) than the rest mixes and this significantly contributed to the observed behaviour.

Overall, the SFRRAC beams showed the highest number of cracks on average, but the intensity of the cracks was much lower compared to those of the other beams. It was also observed that while the cracks developed by the beams containing SF were mostly disjointed upon additional load, those of the beams without SF were typically continuous. Apparently, the presence of SF engendered a more ductile mode of failure.

4.4.3. Load-deflection

Fig. 11 shows the plot of the load at each load step against the corresponding mid-span deflections for both experimental and theoretical values for all the mixes. In theory, according to Megson [76], the deflection (δ) for a simply supported beam loaded as illustrated in Fig. 6 (a) is related to the applied load (P), shear span (x), elastic modulus of concrete (E), and second moment of area of the beam about the neutral axis (I) as follows:

$$\delta = \; = -23Px^3/48EI \tag{6}$$

This relationship was used to obtain the values for the theoretical deflection at the mid-span. The experimental results show that all the

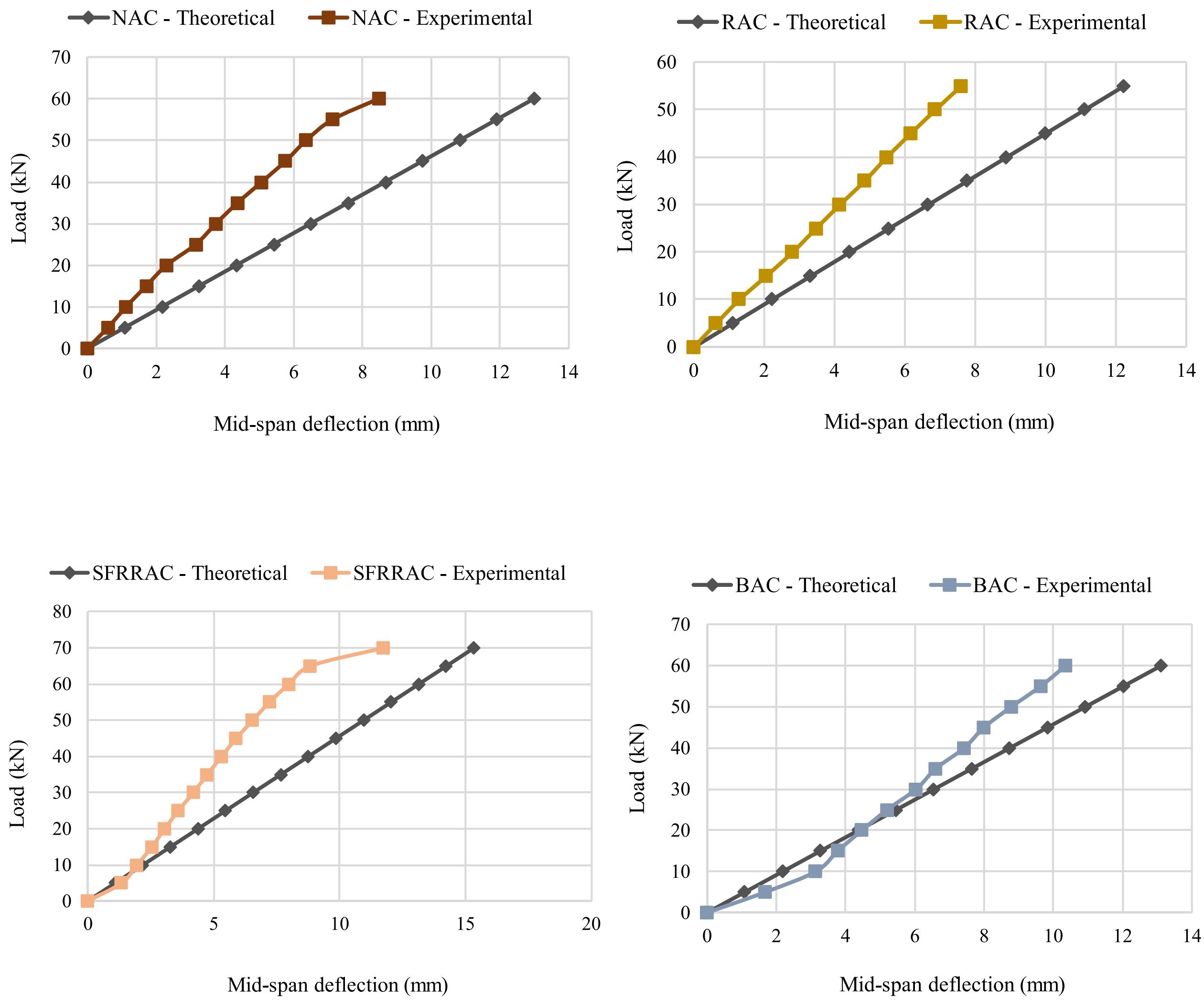

Fig. 11. Experimental and theoretical load–deflection plots obtained at every load-step for the beams from different mixes.

beams produced from mixes proportioned with the conventional method (including the reference mix), exhibited a similar load–deflection behaviour at the mid-span. Consequently, the general theory of bending appropriate for conventional concrete can be applied to the concrete containing RA. Conversely, the BAC beam showed a load–deflection response at variant with the other beams, and this may be linked with the higher coarse aggregate content of the BAC mix. It can also be observed that the difference between the experimental and theoretical load–deflection responses is narrower for the BAC beam than the beam realised from mixes prepared using the conventional method. Furthermore, the load–deflection plots showed that the BAC beam had a higher ductility compared to both NAC and RAC beams and similar ductility with the SFRRAC beam (even with the presence of SF). However, it is important to mention that the elastic modulus of concrete used in this study was estimated according to ACI 318R [89]. Thus, the difference between the observed and calculated values of the deflection is expected to range from 80 to 120% due to mix proportions and elastic modulus of aggregate which affect the elastic modulus of concrete [89]. Generally, the results of this investigation show that the load–deflection responses of the concrete beams containing RA are comparable to that of the conventional beam made of NA.

4.4.4. Strains

Fig. 12 shows the plot of the strains developed in the beams as the loads were applied. Apparently, there is a linear distribution of strain across the depth of the beams. Regardless of aggregate type, the beams produced from the mixes without SF exhibited a similar pattern of strain distribution. Conversely, the beam incorporating SF had a different strain distribution pattern. A maximum strain value of 0.0044 was recorded for both BAC and SFRRAC beams prior to failure, exceeding those of their comparable NAC and RAC beams. The ability of SF to intercept cracks in the SFRRAC beam and the higher volume of coarse aggregate (which also restrained cracks) in the BAC beam, were the factors responsible for the observed result. The points at which the lines of best fit intersect the vertical axis of the plots are referred to as neutral axis depth. It can be noticed in Fig. 12 that the neutral axis position was shifting with increasing load, and it almost stabilized at a higher loading. The results show that the experimental values of the neutral axis depth range from 56–70 mm, 54–70 mm, 50–110 mm, and 52–68 mm for the NAC, RAC, SFRRAC, and BAC beams respectively, measuring from the top of the beams. Their equivalent values from the analytical approach are 50.19 mm, 52.36 mm, 51.23 mm, and 50.97 mm, respectively. These results show a good correlation between the experimental and analytical

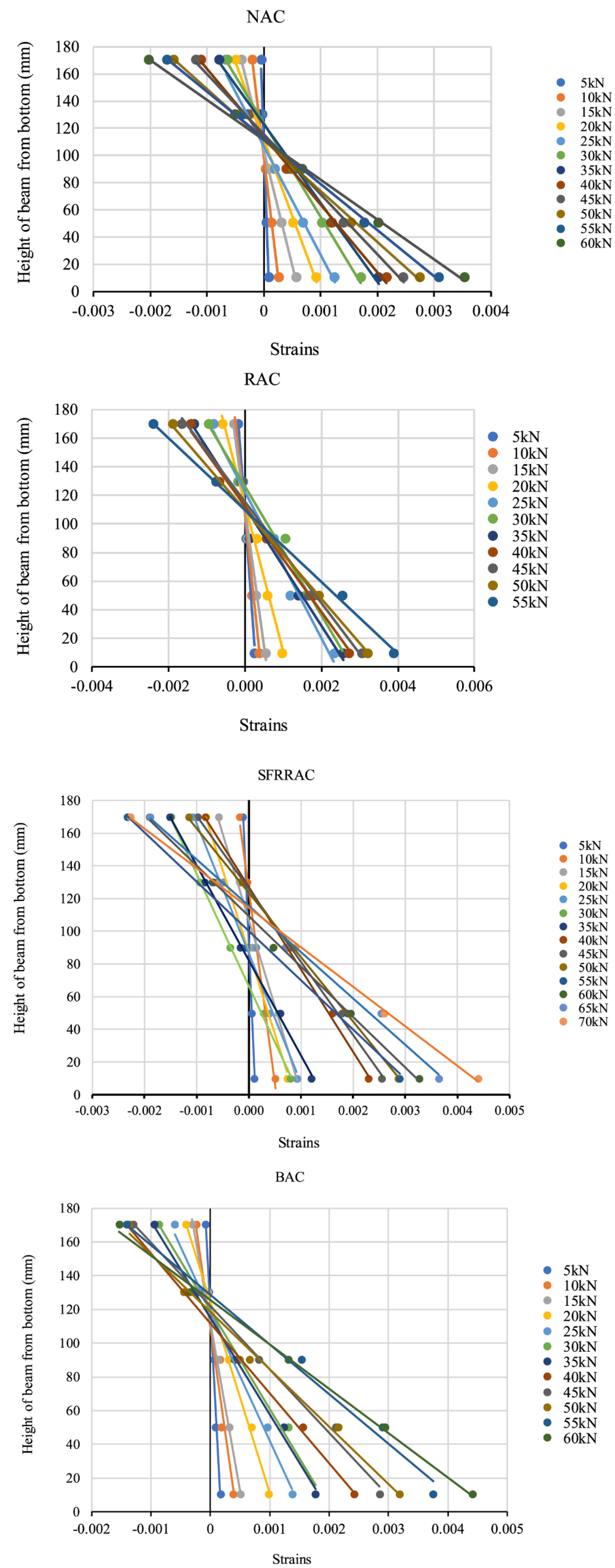

Fig. 12. Strain distribution across the height of the beams produced from different mixes.

investigations.

It should be mentioned that the accuracy of the strain values depends on the placement of the DEMEC buttons at the right positions. This is a difficult task to achieve with 100% accuracy for all the ten DEMEC buttons (as in the current study). Another factor that may have influenced the analytical results is the fact that the elastic modulus of concrete was estimated from a mathematical equation, which ultimately would affect the modular ratio of the composite beam used in determining the neutral axis position. Also, during the casting operation (vibration of concrete), the positions of the reinforcements may have changed due to a possible shift of the spacers, resulting in the alteration of neutral axis positions. However, based on the results of this study, the flexural behaviour of concrete beams containing RA does not vary significantly from that of the conventional concrete beam. Again, the use of the extended EMV mix proportioning approach offsets the requirements for SF in the concrete containing RA and results in low carbon footprint. Therefore, it can be stated that the BAC beam serves as a better replacement for the conventional beam than the SFRRAC beam from both economic and environmental points of view.

5. Conclusions

The flexural performance of reinforced concrete beams containing both recycled coarse aggregate (RCA) and recycled fine aggregate (RFA) with steel fibres (SF) were investigated experimentally and presented in this work. Compressive strength, splitting tensile strength, and hardened density of concrete were also studied. A total of five mixes were formulated using both conventional and alternative mix proportioning methods to evaluate load capacity, crack pattern and development, strain, and mid-span deflection of the beams. The alternative method known as Equivalent mortar volume (EMV) technique, which was developed for RCA, was extended in this study to incorporate RFA, and referred to as extended EMV method. Based on the results of this investigation, the following conclusions were drawn:

- The EMV method can be adapted for RFA in concrete production by applying the same substitution ratio obtained for RCA, with no devastating effects on the mechanical properties of the resulting concrete. However, to attain the desired workability, the slump value of the BAC mix prepared using the extended EMV method varied by up to 35% compared with the reference mix.
- The mechanical properties of concrete were affected by both recycled aggregate content and presence of SF. At full replacement with recycled aggregate, compressive strength and hardened density decreased by up to 21% and 8%, respectively, while the splitting tensile strength increased by about 6% when compared with the reference mix. The influence of SF on splitting tensile strength depended on mix design method, with the conventional and unconventional methods leading to 38% and 10% increase, respectively.
- The SFRRAC beam showed the highest load bearing capacity than the corresponding NAC, BAC, and RAC beams, with about 8%, 8%, and 13% difference, respectively. A similar trend was observed for the moment capacity of the beams.
- Cracks in the NAC, SFRRAC, and BAC beams were initiated at a load of 20kN while those in the RAC beam occurred at a load of 15kN. In terms of crack pattern, the NAC, RAC, and BAC beams were similar, however, the BAC beam showed a relatively lesser severe and fewer number of cracks attributed to greater quantity of coarse aggregate. On the other hand, the SFRRAC beam had the highest number of cracks but were mostly disjointed due to the bridging effect of the SF. At the fracture, the BAC and NAC beams showed the least and highest estimated crack width of 1.0 mm and 4.0 mm, respectively. Therefore, the BAC beam

showed a better performance at serviceability limit state than all the other beams.

- All test beams failed in a ductile manner regardless of aggregate type and mix proportioning method, although the use of SF was of added advantage in this regard. Also, there was a good correlation between the observed and predicted mid-span deflection for both the reference and BAC beams.

Declaration of Competing Interest

The authors declare that they have no known competing financial interests or personal relationships that could have appeared to influence the work reported in this paper.

Acknowledgements

The authors acknowledge the contributions of Litecast Homefloors Limited, Nuneaton, United Kingdom and Dalian HARVEST Metal Fibres Co. Limited, China for supplying the materials used for this research, free of charge.

Appendix A

Example: This illustrates the determination of the theoretical parameters defining the reinforced concrete beams produced from NAC mix. Recall the following:

i. Concrete cover, $C = 20mm$
ii. Area of steel reinforcements (2Y10), $A_s = 157.08mm^2$
iii. Width of beam, $b = 80mm$
iv. Overall depth of beam, $h = 180mm$

Hence, the effective depth of beam, $d = h - C - 0.5 \times \textit{diameter of steel} = 155mm$

v. Shear span of beam, $a = 400mm$
vi. Elastic modulus for concrete, $E_c = 4700\sqrt{f_c}$ where f_c is the compressive strength of the concrete (MPa)
vii. Elastic modulus of steel, E_s

Therefore, the modular ratio, $m = E_{s/E_c} = 210000/34300 = 6.12$

(1) Determining the neutral axis depth, y

From Equation (1), the neutral axis depth, y is given by:

$$y = mA_s/b\left(\sqrt{1 + 2bd/mA_s} - 1\right)$$

Substituting, $y = 6.12 \times 157.08/80\left(\sqrt{1 + 2 \times 80 \times 155/6.12 \times 157.08} - 1\right)$
This gives, $y = 50.19mm$

(2) Determining the moment of inertia, I

From Equation (1), the moment of inertia, I is given by:

$$I = by^3/3 + mA_s(d - y)^2$$

Substituting, $I = 80 \times 50.19^3/3 + 6.12 \times 157.08(155 - 50.19)^2$
This gives, $I = 13931814.41mm^4$.

(3) Determining the moment of resistance, M_r

From Equation (2), M_r is given by:
$M_r = f_c^{`}/2\left[by(d - y/3)\right]$ where $f_c^{`}$ is the cylindrical compressive strength of the concrete.
Substituting, $M_r = 53.3/2 \times 80 \times 50.19(155 - 50.19/3) \times 10^6$
This gives, $M_r = 14.8kNm$

(4) Determining the ultimate load, P_{ult}

From Equation (4), the ultimate load, P_{ult} is given by: $P_{ult} = 2M_r/a$
Substituting, $P_{ult} = 2 \times 14.8/0.4$
This gives, $P_{ult} = 74kN$
Similar procedures were followed to obtain the corresponding values for the RAC, SFRRAC, and BAC beams.

References

[1] Union Européenne des Producteurs de Granulats. EUROPEAN AGGREGATES ASSOCIATION - A Sustainable Industry for A Sustainable Europe. UEPG Annu Rev 2019-2020 2019:1-30 https://uepg.testurl.fr/mediatheque/media/UEP.

[2] Freedonia. Global Construction Aggregates 2019:https://www.freedoniagroup.com/World-Construction-. https://doi.org/p.com/World-Construction-Aggregates.html.

[3] Anike E, Saidani M, Ganjian E, Tyrer M, Olubanwo A. Evaluation of conventional and equivalent mortar volume mix design methods for recycled aggregate concrete. Mater Struct 2020;53:22. https://doi.org/10.1617/s11527-020-1457-3.

[4] Anike EE, Saidani M, Olubanwo AO, Tyrer M. Extended application of the equivalent mortar volume mix design method for recycled aggregate concrete. *World Congr Civil, Struct Environ Eng* 2020;mix:132-1-132–7. doi:10.11159/icsect20.132.

[5] Tabsh SW, Abdelfatah AS. Influence of recycled concrete aggregates on strength properties of concrete. Constr Build Mater 2009;23:1163–7. https://doi.org/10.1016/j.conbuildmat.2008.06.007.

[6] Oikonomou ND. Recycled concrete aggregates. Cem Concr Compos 2005;27:315–8. https://doi.org/10.1016/J.CEMCONCOMP.2004.02.020.

[7] Anike EE, Saidani M, Ganjian E, Tyrer M, Olubanwo AO. The potency of recycled aggregate in new concrete: a review. Constr Innov 2019;19:594–613. https://doi.org/10.1108/CI-07-2018-0056.

[8] Anike EE, Saidani M, Ganjian E, Tyrer M. RECYCLED CONCRETE AGGREGATE AND ITS PROSPECTS IN STRUCTURAL CONCRETE. Young Res. Forum IV Innov. Constr. Mater., 2018, p. 75–8.

[9] Ghalehnovi M, Roshan N, Hakak E, Shamsabadi EA, de Brito J. Effect of red mud (bauxite residue) as cement replacement on the properties of self-compacting concrete incorporating various fillers. J Clean Prod 2019;240:118213. https://doi.org/10.1016/j.jclepro.2019.118213.

[10] Malešev M, Radonjanin V, Broćeta G. The properties of recycled aggregate concrete. Contemp Mater 2014;2:239–49. https://doi.org/10.7251/COMEN1402239M.

[11] Ebrahim Abu El-Maaty Behiry A. Utilization of cement treated recycled concrete aggregates as base or subbase layer in Egypt. Ain Shams Eng J 2013;4:661–73. https://doi.org/10.1016/j.asej.2013.02.005.

[12] Wagih AM, El-Karmoty HZ, Ebid M, Okba SH. Recycled construction and demolition concrete waste as aggregate for structural concrete. HBRC J 2013;9:193–200. https://doi.org/10.1016/j.hbrcj.2013.08.007.

[13] Olorunsogo FT, Padayachee N. Performance of recycled aggregate concrete monitored by durability indexes. Cem Concr Res 2002;32:179–85. https://doi.org/10.1016/S0008-8846(01)00653-6.

[14] Hansen TC. Recycled aggregates and recycled aggregate concrete second state-of-the-art report developments 1945–1985. Mater Struct 1986;19(3):201–46.

[15] Silva RV, de Brito J, Dhir RK. Availability and processing of recycled aggregates within the construction and demolition supply chain: a review. J Clean Prod 2017;143:598–614. https://doi.org/10.1016/j.jclepro.2016.12.070.

[16] Bravo M, De Brito J, Pontes J, Evangelista L. Mechanical performance of concrete made with aggregates from construction and demolition waste recycling plants. J Clean Prod 2015;99:59–74. https://doi.org/10.1016/j.jclepro.2015.03.012.

[17] Rodrigues F, Carvalho MT, Evangelista L, De Brito J. Physical-chemical and mineralogical characterization of fine aggregates from construction and demolition waste recycling plants. J Clean Prod 2013;52:438–45. https://doi.org/10.1016/j.jclepro.2013.02.023.

[18] Silva RV, De Brito J, Dhir RK. Properties and composition of recycled aggregates from construction and demolition waste suitable for concrete production. Constr Build Mater 2014;65:201–17. https://doi.org/10.1016/j.conbuildmat.2014.04.117.

[19] Wardeh G, Ghorbel E, Gomart H. Mix design and properties of recycled aggregate concretes: applicability of Eurocode 2. Int J Concr Struct Mater 2015;9:1–20. https://doi.org/10.1007/s40069-014-0087-y.

[20] Wang L, Wang J, Qian X, Chen P, Xu Y, Guo J. An environmentally friendly method to improve the quality of recycled concrete aggregates. Constr Build Mater 2017;144:432–41. https://doi.org/10.1016/j.conbuildmat.2017.03.191.

[21] Ismail S, Ramli M. Engineering properties of treated recycled concrete aggregate (RCA) for structural applications. Constr Build Mater 2013;44:464–76. https://doi.org/10.1016/j.conbuildmat.2013.03.014.

[22] Tam VWY, Tam CM, Le KN. Removal of cement mortar remains from recycled aggregate using pre-soaking approaches. Resour Conserv Recycl 2007;50:82–101. https://doi.org/10.1016/j.resconrec.2006.05.012.

[23] Akbarnezhad A, Ong KCG, Zhang MH, Tam CT, Foo TWJ. Microwave-assisted beneficiation of recycled concrete aggregates. Constr Build Mater 2011;25:3469–79. https://doi.org/10.1016/j.conbuildmat.2011.03.038.

[24] Mulder E, de Jong TPR, Feenstra L. Closed cycle construction: an integrated process for the separation and reuse of C&D waste. Waste Manag 2007;27:1408–15. https://doi.org/10.1016/j.wasman.2007.03.013.

[25] Shima H, Tateyashiki H, Matsuhashi R, Yoshida Y. An advanced concrete recycling technology and its applicability assessment through input-output analysis. J Adv Concr Technol 2005;3:53–67. https://doi.org/10.3151/jact.3.53.

[26] Katz A. Treatments for the improvement of recycled aggregate. J Mater Civ Eng 2004;16:597–603. https://doi.org/10.1061/(ASCE)0899-1561(2004)16:6(597).

[27] Behera M, Bhattacharyya SK, Minocha AK, Deoliya R, Maiti S. Recycled aggregate from C&D waste & its use in concrete - a breakthrough towards sustainability in construction sector: a review. Constr Build Mater 2014;68:501–16. https://doi.org/10.1016/j.conbuildmat.2014.07.003.

[28] Etxeberria M, Marí AR, Vázquez E. Recycled aggregate concrete as structural material. Mater Struct 2007;40:529–41. https://doi.org/10.1617/s11527-006-9161-5.

[29] Xiao J, Li J, Zhang C. Mechanical properties of recycled aggregate concrete under uniaxial loading. Cem Concr Res 2005;35:1187–94. https://doi.org/10.1016/j.cemconres.2004.09.020.

[30] Dean SW, Liu J, Chen B. Mechanical properties of high strength concrete with field-demolished concrete as aggregates. J ASTM Int 2008;5(10):101650.

[31] Topcu IB, Sengel S. Properties of concretes produced with waste concrete aggregate. Concr Concr Res 2004;34:1307–12. https://doi.org/10.1016/j.cemconres.2003.12.019.

[32] Dhir RK, Limbachiya MC, Leelawat T. Suitability of recycled concrete aggregate for use in BS 5328 designated mixes. Proc Inst Civ Eng, Struct Build 1999;134(3):257–74.

[33] Liang YC, Ye ZM, Vernerey F, Xi Y. Development of processing methods to improve strength of concrete with 100% recycled coarse aggregate. *J Mater Civ Eng* 2013;27. doi:130801045339002.

[34] Tam VWY, Tam CM. Diversifying two-stage mixing approach (TSMA) for recycled aggregate concrete: TSMAsand TSMAsc. Constr Build Mater 2008;22:2068–77. https://doi.org/10.1016/j.conbuildmat.2007.07.024.

[35] Tam VWY, Gao XF, Tam CM. Environmental enhancement through use of recycled aggregate concrete in a two-stage mixing approach. Hum Ecol Risk Assess 2006;12:277–88. https://doi.org/10.1080/10807030500531653.

[36] Vaishali GG, Rao HS. Strength and permeability characteristics of fiber reinforced high performance concrete with recycled aggregates. Asian J Civ Eng 2012;13:55–78.

[37] Gao D, Zhang L, Nokken M. Compressive behavior of steel fiber reinforced recycled coarse aggregate concrete designed with equivalent cubic compressive strength. Constr Build Mater 2017;141:235–44. https://doi.org/10.1016/j.conbuildmat.2017.02.136.

[38] Kang W-H, Ramesh RB, Mirza O, Senaratne S, Tam V, Wigg D. Reliability based design of RC beams with recycled aggregate and steel fibres. Structures 2017;11:135–45. https://doi.org/10.1016/j.istruc.2017.05.002.

[39] Afroughsabet V, Biolzi L, Ozbakkaloglu T. Influence of double hooked-end steel fibers and slag on mechanical and durability properties of high performance recycled aggregate concrete. Compos Struct 2017;181:273–84. https://doi.org/10.1016/j.compstruct.2017.08.086.

[40] Senaratne S, Gerace D, Mirza O, Tam VWY, Kang WH. The costs and benefits of combining recycled aggregate with steel fibres as a sustainable, structural material. J Clean Prod 2016;112:2318–27. https://doi.org/10.1016/j.jclepro.2015.10.041.

[41] Younis KH, Pilakoutas K, Guadagnini M, Angelakopoulos H. Feasibility of Using Recycled Steel Fibres To Enhance the Behaviour of Recycled Aggregate Concrete. In FRC 2014 Jt ACI-Fib Int Work - Fibre Reinf Concr from Des to Struct Appl 2014:113–22.

[42] Graeff ÂG. Long-term performance of recycled steel fibre reinforced concrete for pavement applications. University of Sheffield Sheffield, 2011.

[43] Pilakoutas K, Neocleous K, Tlemat H. Reuse of tyre steel fibres as concrete reinforcement. Proc ICE Eng Sustain 2004;157:131–8. https://doi.org/10.1680/ensu.157.3.131.48644.

[44] Tlemat H. Steel fibres from waste tyres to concrete: testing, modelling and design. UK: The University of Sheffield; 2004. Ph.D. Thesis.

[45] Lim DH, Oh BH. Experimental and theoretical investigation on the shear of steel fibre reinforced concrete beams. Eng Struct 1999;21:937–44. https://doi.org/10.1016/S0141-0296(98)00049-2.

[46] Boulekbache B, Hamrat M, Chemrouk M, Amziane S. Influence of yield stress and compressive strength on direct shear behaviour of steel fibre-reinforced concrete. Constr Build Mater 2012;27:6–14. https://doi.org/10.1016/j.conbuildmat.2011.07.015.

[47] Boulekbache B, Hamrat M, Chemrouk M, Amziane S. Flowability of fibre-reinforced concrete and its effect on the mechanical properties of the material. Constr Build Mater 2010;24:1664–71. https://doi.org/10.1016/j.conbuildmat.2010.02.025.

[48] Erdem S, Dawson AR, Thom NH. Microstructure-linked strength properties and impact response of conventional and recycled concrete reinforced with steel and synthetic macro fibres. Constr Build Mater 2011;25:4025–36. https://doi.org/10.1016/j.conbuildmat.2011.04.037.

[49] Altun F, Haktanir T, Ari K. Effects of steel fiber addition on mechanical properties of concrete and RC beams. Constr Build Mater 2007;21:654–61. https://doi.org/10.1016/j.conbuildmat.2005.12.006.

[50] Lee MK, Barr BIG. An overview of the fatigue behaviour of plain and fibre reinforced concrete. Cem Concr Compos 2004;26:299–305. https://doi.org/10.1016/S0958-9465(02)00139-7.

[51] Abbas A, Fathifazl G, Isgor OB, Razaqpur AG, Fournier B, Foo S. Durability of recycled aggregate concrete designed with equivalent mortar volume method. Cem Concr Compos 2009;31:555–63. https://doi.org/10.1016/j.cemconcomp.2009.02.012.

[52] Fathifazl G, Abbas A, Razaqpur AG, Isgor OB, Fournier B, Foo S. New mixture proportioning method for concrete made with coarse recycled concrete aggregate. J Mater Civ Eng 2009;21:601–11. https://doi.org/10.1061/(ASCE)0899-1561(2009)21:10(601).

[53] Pradhan S, Kumar S, Barai SV. Recycled aggregate concrete: Particle Packing Method (PPM) of mix design approach. Constr Build Mater 2017;152:269–84. https://doi.org/10.1016/j.conbuildmat.2017.06.171.

[54] Fathifazl G, Razaqpur AG, Isgor OB, Abbas A, Fournier B, Foo S. Flexural performance of steel-reinforced recycled concrete beams. ACI Struct J 2009;106:858–67. https://doi.org/10.14359/51663187.

[55] Pradhan S, Kumar S, Barai SV. Performance of reinforced recycled aggregate concrete beams in flexure: experimental and critical comparative analysis. Mater Struct 2018;51(3).
[56] Arezoumandi M, Smith A, Volz JS, Khayat KH. An experimental study on flexural strength of reinforced concrete beams with 100% recycled concrete aggregate. Eng Struct 2015;88:154–62. https://doi.org/10.1016/j.engstruct.2015.01.043.
[57] Ignjatović IS, Marinković SB, Mišković ZM, Savić AR. Flexural behavior of reinforced recycled aggregate concrete beams under short-term loading. Mater Struct 2013;46:1045–59. https://doi.org/10.1617/s11527-012-9952-9.
[58] Ossa A, García JL, Botero E. Use of recycled construction and demolition waste (CDW) aggregates: A sustainable alternative for the pavement construction industry. J Clean Prod 2016;135:379–86. https://doi.org/10.1016/j.jclepro.2016.06.088.
[59] Soares D, De Brito J, Ferreira J, Pacheco J. Use of coarse recycled aggregates from precast concrete rejects: mechanical and durability performance. Constr Build Mater 2014;71:263–72. https://doi.org/10.1016/j.conbuildmat.2014.08.034.
[60] Thomas C, Cimentada A, Polanco JA, Setién J, Méndez D, Rico J. Influence of recycled aggregates containing sulphur on properties of recycled aggregate mortar and concrete. Compos Part B 2013;45:474–85. https://doi.org/10.1016/j.compositesb.2012.05.019.
[61] Thomas C, Setién J, Polanco JA. Structural recycled aggregate concrete made with precast wastes. Constr Build Mater 2016;114:536–46. https://doi.org/10.1016/j.conbuildmat.2016.03.203.
[62] ASTM C136. Standard Test Method for Sieve Analysis of Fine and Coarse Aggregates. 2014. doi:10.1520/C0136_C0136M-14.
[63] ASTM C29/C29M-09. Standard Test Method for Bulk Density (" Unit Weight ") and Voids in Aggregate. 2009. doi:10.1520/C0029_C0029M-17a.
[64] ASTM C128. Standard Test Method for Relative Density (Specific Gravity) and Absorption of Fine Aggregate. 2015. doi:10.1520/C0128-15.
[65] ASTM C127 – 15. Standard Test Method for Relative Density (Specific Gravity) and Absorption of Coarse Aggregate. 2015. doi:10.1520/C0127-15.
[66] BS EN 197-1. Part 1: Composition, specifications and conformity criteria for common cements. 2011.
[67] BS EN 934-2:2009 +A1:2012. Admixtures for concrete , mortar and grout: Part 2: Concrete admixtures — Part 2: Concrete admixtures — Definitions, requirements, conformity, Definitions, requirements, conformity, marking and labelling marking. 2012.
[68] NSCS. National Structural Concrete Specification for Building Construction. Technical Committee. 4th editio. 2010.
[69] BS 8500-1:2015+A2. Concrete- Complementary British Standard to BS EN 206-1; Part 1:Method of specifying and guidance for the specifier. 2019.
[70] ACI Committee 211. ACI 211 1-91 Standard Practice for Selecting Proportions for Normal, Heavyweight, and Mass Concrete. 2009.
[71] Teychenné DC, Franklin RE, Erntroy HC. Design of normal concrete mixes. vol. 331. Second edi. 1997.
[72] Anike EE, Saidani M, Olubanwo AO, Tyrer M, Ganjian E. Effect of mix design methods on the mechanical properties of steel fibre-reinforced concrete prepared with recycled aggregates from precast waste. Structures 2020;27:664–72. https://doi.org/10.1016/j.istruc.2020.05.038.
[73] BS EN 12390-7. Testing hardened concrete Part 7: Density of hardened concrete. vol. 53. 2009. doi:10.1017/CBO9781107415324.004.
[74] BS EN 12390-3. Testing hardened concrete- Part3: Compressive strength of test specimens 2009;3:1–19.
[75] BS EN 12390-6. Testing hardened concrete- Part 6: Tensile splitting strength of test specimens. vol. 3. 2009.
[76] Megson THG. Structural and Stress Analysis. 3rd edn. Oxford: Elsevier Ltd.; 2014.
[77] Punmia BC, Jain AK, Jain AK. REINFORCED CONCRETE. STRUCTURES. vol. II. fifth. Laxmi Publications Ltd; 1992.
[78] Evangelista L, de Brito J. Mechanical behaviour of concrete made with fine recycled concrete aggregates. Cem Concr Compos 2007;29:397–401. https://doi.org/10.1016/j.cemconcomp.2006.12.004.
[79] Poon CS, Shui ZH, Lam L, Fok H, Kou SC. Influence of moisture states of natural and recycled aggregates on the slump and compressive strength of concrete. Cem Concr Res 2004;34:31–6. https://doi.org/10.1016/S0008-8846(03)00186-8.
[80] Kurad R, Silvestre JD, de Brito J, Ahmed H. Effect of incorporation of high volume of recycled concrete aggregates and fly ash on the strength and global warming potential of concrete. J Clean Prod 2017;166:485–502. https://doi.org/10.1016/j.jclepro.2017.07.236.
[81] Kou SC, Poon CS, Chan D. Influence of fly ash on the properties of recycled coarse aggregate concrete. J Mater Civ Eng 2007;19:709–17. https://doi.org/10.1061/(ASCE)0899-1561 (2007) 19:9(709).
[82] Moosberg-Bustnes H, Lagerblad B, Forssberg E. The function of fillers in concrete. Mater Struct Constr 2004;37:74–81. https://doi.org/10.1617/13694.
[83] Gupta PK, Bhatia R. Study of engineering properties of recycled concrete aggregate concrete. I-Manager's. J Struct Eng 2013;2:20–7.
[84] Andreu G, Miren E. Experimental analysis of properties of high performance recycled aggregate concrete. Constr Build Mater 2014;52:227–35. https://doi.org/10.1016/j.conbuildmat.2013.11.054.
[85] Malešev M, Radonjanin V, Marinković S. Recycled concrete as aggregate for structural concrete production. Sustainability 2010;2:1204–25. https://doi.org/10.3390/su2051204.
[86] Etxeberria M, Vázquez E, Marí A, Barra M. Influence of amount of recycled coarse aggregates and production process on properties of recycled aggregate concrete. Cem Concr Res 2007;37:735–42. https://doi.org/10.1016/j.cemconres.2007.02.002.
[87] Akinkurolere OO. Experimental investigation on the influence of steel fiber on the compressive and tensile strength of recycled aggregate concrete. J Eng Appl Sci 2010;5:264–8. https://doi.org/10.3923/jeasci.2010.264.268.
[88] Kumar PS, Mannan MA, Kurian VJ, Achuytha H. Investigation on the flexural behaviour of high-performance reinforced concrete beams using sandstone aggregates. Build Environ 2007;42:2622–9. https://doi.org/10.1016/j.buildenv.2006.06.015.
[89] ACI 318R. ACI 318R-14 Building Code Requirements for Structural Concrete. 2014.